Activation of the Unfolded Protein Response Occurs at All Stages of Atherosclerotic Lesion Development in Apolipoprotein E–Deficient Mice

Ji Zhou, MD, PhD*; Šárka Lhoták, PhD*; Brooke A. Hilditch, BSc; Richard C. Austin, PhD

Background—Apoptotic cell death contributes to atherosclerotic lesion instability, rupture, and thrombogenicity. Recent findings suggest that free cholesterol (FC) accumulation in macrophages induces endoplasmic reticulum (ER) stress/unfolded protein response (UPR) and apoptotic cell death; however, it is not known at what stage of lesion development the UPR is induced in macrophages or whether a correlation exists between UPR activation, FC accumulation, and apoptotic cell death.

Methods and Results—Aortic root sections from apolipoprotein E–deficient (apoE$^{-/-}$) mice at 9 weeks of age (early-lesion group) or 23 weeks of age (advanced-lesion group) fed a standard chow diet were examined for markers of UPR activation (GRP78, phospho-PERK, CHOP, and TDAG51), apoptotic cell death (TUNEL and cleaved caspase-3), and lipid accumulation (filipin and oil red O). UPR markers were dramatically increased in very early intimal macrophages and in macrophage foam cells from fatty streaks and advanced atherosclerotic lesions. Although accumulation of FC was observed in early-lesion–resident macrophage foam cells, no evidence of apoptotic cell death was observed; however, UPR activation, FC accumulation, and apoptotic cell death were observed in a small percentage of advanced-lesion–resident macrophage foam cells.

Conclusions—UPR activation occurs at all stages of atherosclerotic lesion development. The additional finding that macrophage apoptosis did not correlate with UPR activation and FC accumulation in early-lesion–resident macrophages suggests that activation of other cellular mediators and/or pathways are required for apoptotic cell death. **(*Circulation*. 2005;111:1814-1821.)**

Key Words: immunohistochemistry ■ atherosclerosis ■ cholesterol ■ apoptosis

Atherosclerosis is a complex, chronic process that results in the formation of stratified lesions of the arterial wall.[1–3] Lipid deposition in the subendothelial cell space, endothelial cell dysfunction, infiltration of monocytic cells, proliferation and migration of smooth muscle cells (SMCs), and elaboration of extracellular matrix are hallmark features of atherosclerotic lesions. Lipid-laden macrophages are observed at all stages of lesion development.[1,3]

It is well established that the acute clinical manifestations of atherosclerosis result from plaque rupture, thereby triggering thrombus formation and vessel occlusion.[4–6] Apoptotic cell death has been well documented in both animal and human atherosclerotic lesions.[7–9] Although the majority of apoptotic cells in the atherosclerotic lesion consist of macrophages, SMCs and endothelial cells also undergo apoptotic cell death. Given these findings, it has been suggested that apoptotic cell death increases the risk of lesion rupture by decreasing the number of viable SMCs necessary for collagen production and stabilization of the fibrous cap. Furthermore, apoptosis enhances thrombogenicity by increasing the number of tissue factor–rich apoptotic cells within the atherosclerotic lesion.[10,11]

Although oxidized LDL and inflammatory factors are know to induce macrophage apoptosis,[12,13] other cellular mediators, including p53,[14] tumor necrosis factor-α,[15] Bax,[16] and Fas ligand,[17] can contribute to the induction of macrophage apoptosis. Lipid analyses at various stages of human and animal atherosclerotic lesion development also demonstrate a steady increase in free cholesterol (FC) with a concomitant decrease in cholesterol ester content during lesion progression.[18,19] Accumulation of FC in macrophage foam cells is thought to be an important process in the progression of atherosclerotic lesions.[20–22] Feng et al[23] reported that accumulation of FC in the endoplasmic reticulum (ER) membrane induces ER stress and activation of the unfolded protein response (UPR) in cultured peritoneal mac-

Received July 12, 2004; revision received November 9, 2004; accepted December 1, 2004.

From the Department of Pathology and Molecular Medicine, McMaster University, and the Henderson Research Centre, Hamilton, Ontario, Canada.

The online-only Data Supplement, which contains Figures I through VI, can be found with this article at http://www.circulationaha.org.

*Drs Zhou and Lhoták contributed equally to this work.

Correspondence to Richard C. Austin, PhD, Henderson Research Centre, 711 Concession St, Hamilton, Ontario L8V 1C3, Canada. E-mail raustin@thrombosis.hhscr.org

Circulation **is available at http://www.circulationaha.org** **DOI: 10.1161/01.CIR.0000160864.31351.C1**

rophages, which leads to apoptotic cell death. In advanced atherosclerotic lesions of apolipoprotein (apo) $E^{-/-}$ mice, FC accumulation correlated with the expression of CHOP (C/EBP homologous protein-10), an ER stress-response gene and member of the CCAAT/enhancer-binding protein (C/EBP) gene family of transcription factors having proapoptotic characteristics.[24] However, it is not known at what stage of lesion development the UPR is induced or whether a temporal relationship exists between FC accumulation, UPR activation, and apoptotic cell death in macrophages in vivo.

In the present investigation, spontaneous atherosclerotic lesions from the aortic root of apo$E^{-/-}$ mice at 9 weeks of age (early-lesion group) or 23 weeks of age (advanced-lesion group) fed a standard chow diet were assayed for markers of ER stress/UPR activation, cholesterol accumulation, and apoptotic cell death. We show that the UPR is activated in very early intimal macrophages, even before a significant accumulation of intracellular FC. Although UPR activation and accumulation of FC were observed in macrophage foam cells from early lesions, there was no evidence of apoptotic cell death. The observation that UPR activation, FC accumulation, and apoptotic cell death only occurred in advanced atherosclerotic lesions suggests that the activation of additional cellular mediators and/or pathways is likely required for macrophage apoptosis.

Methods

Tissue

Female apo$E^{-/-}$ mice on a C57BL/6J background (Jackson Laboratory) were fed a normal chow diet and euthanized at 9 weeks of age (early-lesion group, n=12) or 23 weeks of age (advanced-lesion group, n=12). After blood was obtained from the right ventricle under isoflurane anesthesia, mice were euthanized by cervical dislocation and immediately perfused with 10% buffered formalin. The heart (including the aortic root) was removed, cut transversely,[25] and embedded in paraffin. For frozen sections, unfixed hearts were embedded in OCT (Fisher Scientific) and frozen in liquid nitrogen–cooled isopentane (Sigma). The McMaster University Animal Research Ethics Board approved all procedures.

Immunohistochemistry

From paraffin blocks, 4-μm-thick serial sections were cut through the aortic root. Sections were deparaffinized, and the endogenous peroxidase activity was blocked with 0.5% H_2O_2 in methanol for 10 minutes. For some antibodies, antigen retrieval was performed, as specified below. After blocking with 5% normal goat or rabbit serum, sections were incubated with primary antibody for 1 hour at room temperature, followed by goat anti-rabbit, rabbit anti-rat, or rabbit anti-goat biotinylated secondary antibodies (Vector Laboratories), diluted 1/500 in 0.05 mol/L Tris buffer, pH 7.5, for 30 minutes, and streptavidin-peroxidase (Zymed Laboratories), diluted 1/20, for 5 minutes. Sections were developed in Nova Red peroxidase substrate (Vector Laboratories) and counterstained with hematoxylin. Unless otherwise indicated, nonspecific immunostaining was not detected in sections stained with nonimmune IgG as the primary antibody or with the secondary antibody alone (Data Supplement Figure I).

Double Immunofluorescence

Paraffin sections were deparaffinized, and antigen retrieval was performed when needed (see below). After blocking with 5% normal donkey serum (Chemicon International), sections were incubated with the first primary antibody, followed by the second primary antibody, for 1 hour each. A mix of donkey anti-rabbit or anti-mouse Alexa 488 and donkey anti-goat Alexa 594 (Molecular Probes), diluted 1/200, was applied for 30 minutes. Slides were mounted with Permafluor (Fisher Scientific) and viewed in a Zeiss Axioplan fluorescence microscope.

Antibodies for Immunohistochemistry

Rabbit anti-phospho-PKR-like ER kinase (PERK) (#3191) and anti-cleaved caspase-3 (#9661) antibodies were from Cell Signaling and were used at 1/100 dilution. For cleaved caspase-3, heat-induced epitope retrieval (HIER) was performed for 30 minutes at 95°C in citrate buffer, pH 6.0. Polyclonal antibodies specific for glucose-regulated protein (GRP) 78 (sc-1050), CHOP (sc-575), or T-cell death-associated gene 51 (TDAG51) (sc-6143) were from Santa Cruz Biotechnology. Anti-GRP78 was diluted 1/40 and used without antigen retrieval, and anti-TDAG51 was used at 1/20 dilution after antigen retrieval for 10 minutes at room temperature in 0.05% protease (Sigma). Rabbit anti-CHOP polyclonal antibody (Santa Cruz, sc-575), diluted 1/40, was used after heat retrieval in Retrieve-all 2 (Signet Laboratories) at 95°C for 30 minutes and a 10-minute incubation in 0.1% Triton X. Using kidney sections from tunicamycin-injected wild-type or CHOP$^{-/-}$ mice (kindly provided by Dr I. Tabas, Columbia University, New York, NY), we confirmed that this technique provides authentic CHOP nuclear staining, whereas cytoplasmic staining can be considered as background.

Mac-3 rat monoclonal antibody (clone M3/84, Pharmingen) was used at 1/10 000 dilution after HIER, and rabbit anti-human Von Willebrand factor (DakoCytomation) was used at 1/500 dilution after a protease treatment, as above. Mouse anti-α-smooth muscle actin antibody (A2547; Sigma) was biotinylated with the DAKO-ARK kit (DakoCytomation) and visualized with streptavidin-peroxidase and Nova Red as described above.

Filipin, Oil Red O, and Terminal dUTP Nick End-Labeling Staining

For filipin and oil red O staining, 5-μm-thick cryostat sections were collected on slides and fixed in 4% paraformaldehyde in 0.1 mol/L phosphate buffer, pH 7.4. Two micrograms of filipin complex (Sigma) was dissolved in 5 μL of DMSO, diluted with 500 μL of PBS, and used immediately. Sections were incubated for 1 hour, mounted in Permafluor, and viewed in fluorescence microscope under ultraviolet light. For neutral lipid visualization, sections were rinsed in 70% ethanol and incubated in a saturated, filtered solution of oil red O (Sigma) in 70% ethanol for 1 hour. After a rinse in 70% ethanol, nuclei were stained with hematoxylin, and slides were mounted in Permafluor. For terminal dUTP nick end-labeling (TUNEL) staining, tissues were pretreated with 3% citric acid for 1 hour to minimize nonspecific staining,[26] followed by the TUNEL procedure with the TACS 2 Apoptosis Detection kit (BIO/CAN Scientific). The incorporated biotinylated nucleotides were visualized with streptavidin-peroxidase and Nova Red substrate as described in the Immunohistochemistry section.

Morphometry

The number of lesional cells per slide, immunostained for GRP78, phospho-PERK, TDAG51, cleaved caspase-3, or TUNEL, were counted and expressed as a percentage of the total lesional macrophages.

Immunoblot Analysis

Mice from the early- or advanced-lesion groups were randomly selected and euthanized, and the aortas were dissected. Total tissue protein lysates from the aortas were solubilized in SDS-PAGE sample buffer, separated on 10% SDS-polyacrylamide gels, and transferred electrophoretically onto nitrocellulose membranes, as described previously.[27] After incubation with primary antibodies to GRP78 (610978; BD Transduction Laboratories), CHOP (sc-575; Santa Cruz), or XBP-1 (m-186; Santa Cruz), followed by horseradish peroxidase–conjugated secondary antibodies, the membranes were developed with the chemiluminescent substrate and exposed to

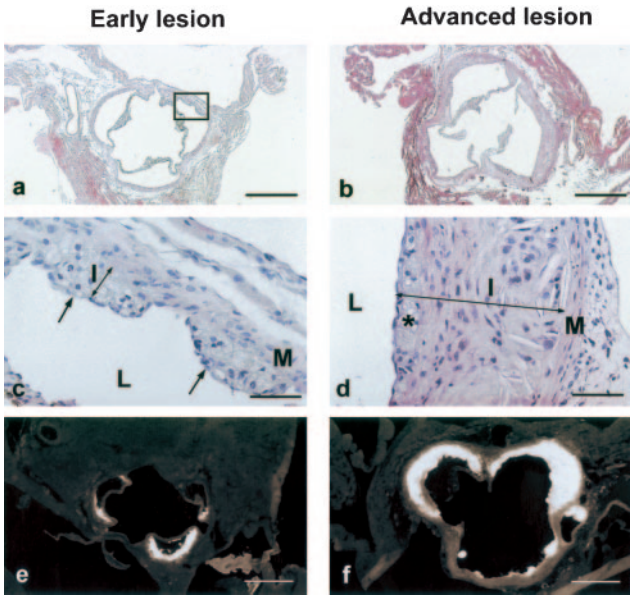

Figure 1. Characterization of early and advanced atherosclerotic lesions in apoE$^{-/-}$ mice. Hematoxylin-and-eosin staining of sections from aortic root of apoE$^{-/-}$ mice with early (a and c) or advanced (b and d) lesions. Intimal fatty streaks composed of foam cells were observed in early lesions (arrows in c). In advanced lesions, necrotic core containing cholesterol crystals at base of intima was overlaid by SMC cap and layer of foam cells (asterisk in d). Filipin staining showed FC accumulation in foam cells from early lesions (e) and throughout lesions both in necrotic acellular areas and in foam cells from advanced lesions (f). I indicates intima; M, media; and L, lumen. Inserted box in Figure 1a is shown in Figure 1c. Bar=500 μm in a, b, e, and f. Bar=50 μm in c and d.

Kodak X-OMAT film. Control for equivalent protein loading was assessed with an anti-β-actin antibody (A5441; Sigma).

Results

Characterization of Atherosclerotic Lesions in the Aortic Root of ApoE$^{-/-}$ Mice

Paraffin sections from the aortic root of apoE$^{-/-}$ mice either 9 (early-lesion group, n=12) or 23 (advanced-lesion group, n=12) weeks of age that were fed a normal chow diet were stained with hematoxylin and eosin to assess lesion growth and gross cellular morphology (Figure 1, a through d). Mean atherosclerotic lesion size was significantly larger in the advanced-lesion group than the early-lesion group (256.7±75.9 $\mu m^2\times10^3$ versus 7.3±2.9 $\mu m^2\times10^3$, $P<0.001$; Figure 1, b versus a). In the early-lesion group, fatty streaks were composed of lipid-enriched cells (Figure 1c). Acellular necrotic areas were not observed at this stage. In the advanced-lesion group, the intima consisted of a necrotic lipid core with cellular debris and a cellular/fibrous cap (Figure 1d). Stretches of simple fatty streaks or individual intimal macrophages were also observed adjacent to these complex lesions (not shown). In frozen sections of early lesions, lipid-enriched foam cells stained intensely for filipin, a marker of FC (Figure 1e). Consistent with the increased mean atherosclerotic lesion size, filipin staining was markedly increased in both the necrotic regions and adjacent intact cells in the advanced-lesion group (Figure 1f).

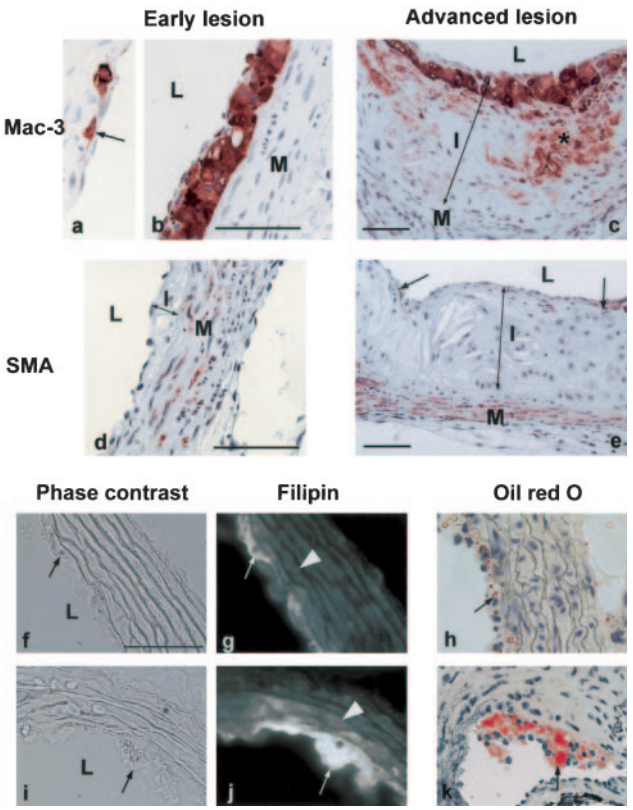

Figure 2. Cellular composition of lesions and lipid accumulation in early lesional macrophages. Immunolabeling with Mac-3 antibody in intimal macrophages (arrow in a) and foam cells in fatty streaks (b). In advanced lesions, Mac-3 staining was observed in necrotic core (asterisk in c) and in foam cells overlaying lesion on luminal side (c). Immunostaining for α-smooth muscle actin was observed in media but not intima of early lesions (d). In advanced lesions, SMCs were present in cap (arrows in e). Intimal macrophage identified by round nucleus (arrows in f and g) and macrophage foam cell containing lipid droplets (arrows in i and j) were observed in phase contrast (f and i) and filipin staining (g and j). Filipin staining in underlying SMCs is indicated by arrowheads. Neutral lipids were visualized by oil red O staining in intimal and macrophage foam cells (arrows in h and k). I indicates intima; M, media; and L, lumen. Bar=50 μm.

Identification of Macrophages and SMCs in Early and Advanced Atherosclerotic Lesions

Lesional macrophages were identified by immunostaining with a Mac-3 antibody (Figure 2, a through c), whereas SMCs were identified with an α-smooth muscle actin antibody (Figure 2, d and e). In the early-lesion group, Mac-3 immunostaining revealed the presence of intimal macrophages as individual elongated cells with round nuclei (Figure 2a). Fatty streaks were found to be composed of lipid-enriched Mac-3 positive macrophage foam cells (Figure 2b). In the advanced-lesion group, macrophage foam cells in the cap region and cellular debris within the lipid-rich necrotic core stained for Mac-3 (Figure 2c). In contrast to macrophages, SMCs were found exclusively in the media of early lesions (Figure 2d). In advanced lesions, intact SMCs were observed in both the media and cap region (Figure 2e).

To further characterize the macrophages in the early lesions, we investigated lipid composition by staining frozen sections with filipin for FC and with oil red O for cholesterol

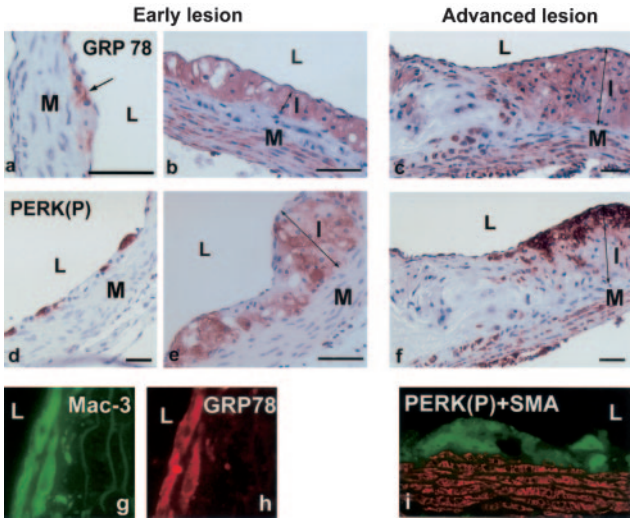

Figure 3. Identification of GRP78 and phospho-PERK in early and late atherosclerotic lesions. Intimal macrophages (arrow in a) and macrophage foam cells in fatty streaks (b) immunostained for GRP78. Majority of cells within advanced lesion were positive for GRP78 (c). In some fatty streaks and advanced lesions, SMCs in media were also immunopositive for GRP78 (b and c). Phospho-PERK immunostaining was similar to that of GRP78 (d to f) except that phospho-PERK staining was absent in medial SMCs underlying early lesions (d and e). Colocalization of Mac-3 (g) and GRP78 (h) is shown in early intimal macrophages. Phospho-PERK (green) and α-smooth muscle actin (SMA; red) did not colocalize in fatty streaks from early lesions (i). I indicates intima; M, media; and L, lumen. Bar=50 μm.

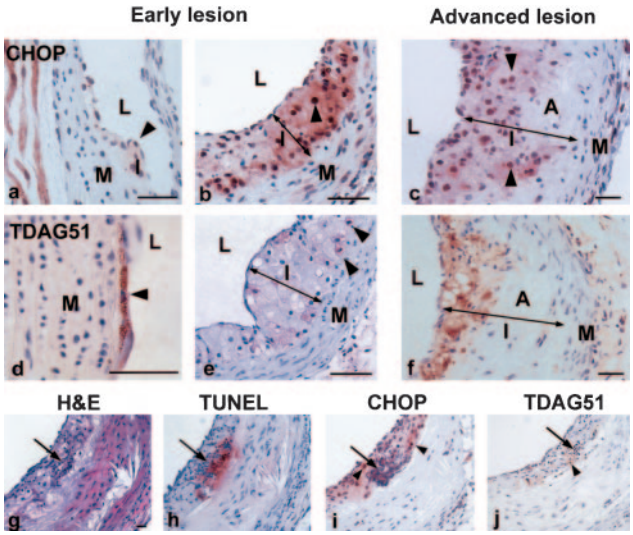

Figure 4. Identification of CHOP and TDAG51 in early and late atherosclerotic lesions. Weak CHOP immunostaining was observed in intimal macrophages (arrowhead in a). Prominent nuclear staining (arrowheads) of CHOP was observed in macrophage foam cells in fatty streaks (b) and cells in cellular portion of advanced lesion (c). TDAG51 was observed in intimal macrophages (arrowhead in d), macrophage foam cells in fatty streaks (e), and cellular part of advanced lesion (f). Staining for both CHOP and TDAG51 was absent from acellular necrotic areas (c and f). Consecutive sections of advanced lesion stained with hematoxylin and eosin (H&E; g) and TUNEL (h) and immunostained for CHOP (i) and TDAG51 (j). Apoptotic region identified by nuclear fragmentation (arrow in g to j) is positive for TUNEL (h). I indicates intima; M, media; L, lumen; and A, acellular necrotic core. Bar=50 μm.

esters. In the intimal macrophages, FC content was only slightly higher by filipin staining than in adjacent SMCs (Figure 2, f and g), and small droplets of neutral lipids were seen by oil red O staining in these cells (Figure 2h). In fatty streaks, marked accumulation of FC and large droplets of neutral lipids were observed in macrophage foam cells (Figure 2, i through k).

Identification of ER Stress/UPR Markers in Early and Advanced Atherosclerotic Lesions

Expression of ER stress and UPR markers, including GRP78, phospho-PERK, CHOP, and TDAG51, were assessed from 3 stages of lesional macrophage progression: (1) intimal macrophages, (2) macrophage foam cells within the fatty streak, and (3) macrophage foam cells in complex lesions (Figures 3 and 4; Data Supplement Figure II). In the early-lesion group, GRP78 staining was observed in 79.3±7.3% of intimal cells, which included both intimal macrophages (Figure 3a) and macrophage foam cells (Figure 3b). The identity of these GRP78-positive cells as macrophages was confirmed by double immunofluorescence for GRP78 and Mac-3 (Figure 3, g and h). Consistent with our previous findings,[28] medial SMCs also stained positive for GRP78 (Figure 3b). In advanced lesions, macrophage foam cells and SMCs were also positive for GRP78 (Figure 3c). Immunostaining for the ER chaperones calreticulin and protein disulphide isomerase also exhibited patterns very similar to GRP78 (Data Supplement Figure III). Phospho-PERK staining was observed at all stages of lesional macrophage development (Figure 3, d through f), including intimal macrophages (Figure 3d). Unlike GRP78, medial SMCs were negative for phospho-PERK in the early lesions (Figure 3, d, e, and i). The staining of phospho-PERK, however, was not uniform in macrophages, and only 33.6±21.9% of the intimal macrophages were found to be positive for phospho-PERK in the early-lesion group. In the advanced lesion, cells within the cap were strongly positive for phospho-PERK (Figure 3f). SMCs were occasionally positive for phospho-PERK, usually below an advanced lesion (Figure 3f).

CHOP/GADD153 is an established marker of ER stress and a member of the C/EBP gene family of transcription factors with proapoptotic characteristics.[24] We observed weak nuclear CHOP immunostaining in some intimal macrophages that showed no morphological signs of apoptosis (Figure 4a). Immunostaining was more pronounced in the macrophage foam cells of fatty streaks that showed a strong nuclear signal (Figure 4b). In advanced lesions, strong cytoplasmic and nuclear staining was observed in intact cells within the lesion (Figure 4c); the acellular necrotic areas, however, were relatively devoid of CHOP staining.

TDAG51 was identified in our laboratory as an ER stress-inducible protein that promotes detachment-mediated apoptotic cell death.[29] Similar to CHOP, we observed TDAG51 staining in intimal macrophages (Figure 4d). In fatty streaks, TDAG51 was observed in macrophage foam cells (Figure 4e); individual cells within a fatty streak stained with a varying degree of intensity, similar to that of phospho-PERK. By morphometry, 38.1±13.3% of intimal cells were

TDAG51-positive in the early lesions. In advanced lesions, intact cells were stained, whereas acellular necrotic areas were devoid of staining (Figure 4f). Only rarely, an apoptotic region characterized by nuclear fragmentation was observed on hematoxylin-and-eosin sections (Figure 4g). In Figure 4g through 4j, adjacent sections through such a region from the advanced lesion are shown. The apoptotic core seen on the hematoxylin-and-eosin–stained section was labeled positively by the TUNEL technique. Although the necrotic core itself was negative for CHOP and TDAG51 immunostaining, CHOP-positive nuclei and TDAG51 cytoplasmic staining were observed in some adjacent macrophages.

To assess whether increased atherosclerotic lesion size correlated with increased expression of ER stress/UPR markers, immunoblot analysis of total aortic tissue lysates was performed. A 2.0-fold increase in the expression of GRP78 was observed in the advanced-lesion group compared with the early-lesion group (Figure 5a). CHOP expression was markedly increased in the advanced-lesion group (Figure 5b). We also examined whether the increased expression of GRP78 and CHOP resulted from the induction of XBP-1, a transcriptional activator known to amplify the expression of these genes after ER stress/UPR activation.[30,31] Indeed, both the spliced (active) and unspliced (latent) forms of the XBP-1 protein were increased in the advanced-lesion group compared with the early-lesion group (Figure 5c).

Identification of Apoptotic Cell Death in Early and Advanced Atherosclerotic Lesions

In the early-lesion group, intimal macrophages and macrophage foam cells within fatty streaks were negative for TUNEL staining (Figure 6a). TUNEL-positive staining was observed occasionally in the necrotic core of advanced lesions (Figure 6b); by morphometry, positive cells represented only 1.2±0.5% of macrophages in the advanced lesion. These results correspond to those reported by other investigators and probably reflect the rapid rate of apoptosis in the lesions.[7] Similar to TUNEL staining, cleaved caspase-3 immunostaining was not observed in intimal macrophages or macrophage foam cells in fatty streaks (Figure 6c) despite UPR activation and FC accumulation in these cells. Cleaved caspase-3 immunostaining was observed in only 0.8±0.7% of all lesional macrophages in the advanced lesions, usually at the base of the necrotic core (Figure 6d). TUNEL staining usually coincided with areas that contained fragmented nuclei. Cleaved caspase-3 immunostaining colocalized with some but not all of these regions (Data Supplement Figure IV). To ascertain that our techniques were functional, controls were performed on sections of mouse thymus that contained a large number of apoptotic thymocytes. Both the TUNEL assay and the cleaved caspase-3 immunostaining labeled cells with apoptotic morphology (Data Supplement Figure V).

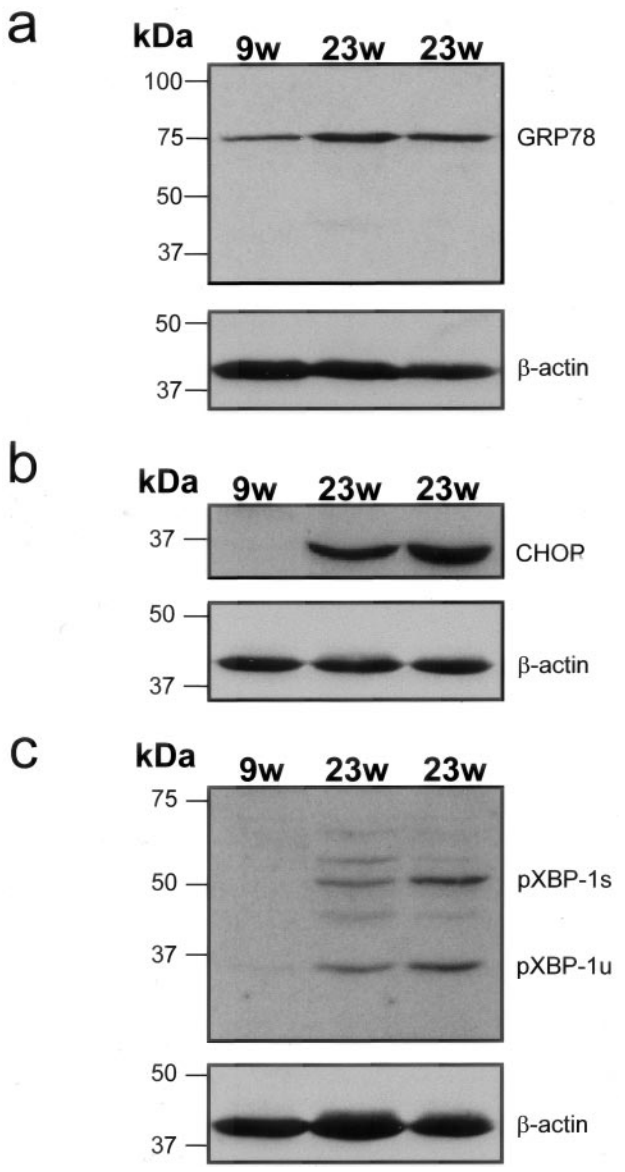

Figure 5. Immunoblot analysis for GRP78, CHOP, and XBP-1 in aortic tissue lysates. Lysates from representative aortas of 9-week-old (9w) or 23-week-old (23w[a] and 23w[b]) apoE$^{-/-}$ mice were separated on 10% SDS-polyacrylamide gels, transferred to nitrocellulose membranes, and immunoblotted for GRP78 (a), CHOP (b) or spliced (XBP-1s) and unspliced (XBP-1u) protein forms of XBP-1 (c). To control for protein loading, immunoblots were reprobed with anti-β-actin antibodies.

Discussion

We[32,33] and others[34,35] have demonstrated a causal relationship between hyperhomocysteinemia, a strong and independent risk factor for cardiovascular disease,[36,37] and accelerated atherosclerosis in apoE$^{-/-}$ mice. Furthermore, we have reported that homocysteine induces ER stress and UPR activation in vitro,[38] thereby inducing 3 fundamental processes that contribute to the development of atherothrombosis, namely, lipid dysregulation,[27] apoptotic cell death,[29,39] and enhanced tissue factor activity.[40] The additional observation that multiple cellular stress pathways, including ER stress, are associated with accelerated atherosclerosis in hyperhomocysteinemic apoE$^{-/-}$ mice,[28] as well as the finding that cholesterol-induced ER stress increases macrophage apoptosis and contributes to atherogenesis,[23] suggests that different cardiovascular risk factors induce ER stress and provides evidence for a model linking ER stress and atherothrombotic disease. It is well known that apoE plays an

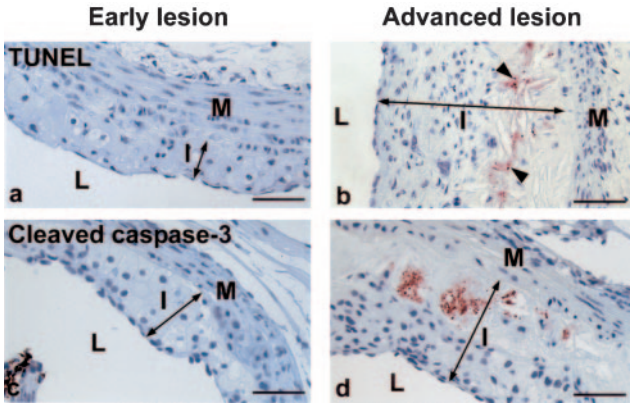

Figure 6. Assessment of apoptotic cell death in early and late atherosclerotic lesions by TUNEL assay and cleaved caspase-3. No evidence of apoptotic cell death, as measured by TUNEL or cleaved caspase-3 staining, was found in early lesions (a and c). TUNEL staining of nuclear fragments (arrowheads in b) or cleaved caspase-3 (d) staining was occasionally observed in the necrotic core of advanced lesions. I indicates intima; M, media; and L, lumen. Bar=100 μm.

important role in macrophage cholesterol efflux. Therefore, apoE$^{-/-}$ mice were selected as a model to investigate the relationship between FC accumulation, UPR activation, and macrophage survival and apoptosis in vivo.

We observed that markers of ER stress and UPR activation were induced dramatically in macrophages from all stages of atherosclerotic development in apoE$^{-/-}$ mice fed a standard chow diet. In the very early intimal macrophages, UPR activation precedes any significant FC accumulation, which suggests that other pathophysiological conditions involved in lesion development, in addition to FC and hyperhomocysteinemia, can activate the UPR in macrophages. Although we have not yet identified these conditions, several possibilities exist. Recent studies have demonstrated that differentiation of B cells to plasma cells requires XBP-1.[41] One of the first observable changes in the artery wall is the transmigration of monocytes into the intima, where they proliferate and differentiate into macrophages. After differentiation, macrophages endocytose lipoproteins and eventually become lipid-laden macrophage foam cells.[42] Thus, it is possible that the binding of monocytes to the endothelium and their subsequent differentiation into macrophages and eventually foam cells may require XBP-1, thereby accounting for the UPR activation. In support of this concept, markers of UPR activation, including XBP-1, are increased in cultured human peripheral blood monocytes when differentiated into macrophages (Data Supplement Figure VI). Peroxynitrite and nitric oxide can induce ER stress in cultured neuronal and pancreatic cell lines, resulting in cell dysfunction and apoptosis.[43,44] As reported recently, 3-nitrotyrosine staining, which indicates the presence of peroxynitrite, precisely colocalizes with macrophages in atherosclerotic lesions from apoE$^{-/-}$ mice.[45] Consistent with these findings, we have demonstrated that peroxynitrite causes endothelial cell apoptosis through a mechanism that involves ER stress and that 3-nitrotyrosine staining colocalizes with UPR markers in early-lesion–resident macrophages from apoE$^{-/-}$ mice (J.G. Dickhout, PhD, and R.C. Austin, PhD, submitted for publication, 2005). Tumor-resident macrophages in the vicinity of viable tumor cells and necrotic areas also have increased UPR activation, as shown by a high level of β-galactosidase transgene expression driven by the GRP94 promoter.[46] Given that the GRP94 promoter is primarily activated by glucose starvation or altered metabolic state within the tumor microenvironment, similar nutritional/metabolic deficiencies could also contribute to UPR activation in lesion-resident macrophages.

Accumulation of FC and lipid droplets was evident in the majority of macrophage foam cells from fatty streaks and advanced lesions. Normally, intracellular cholesterol levels are highly regulated. Macrophages are protected from the accumulation of excess FC by esterification, cholesterol efflux, and the controlled storage and/or hydrolysis of cholesterol esters; however, during atherosclerotic lesion development, lipoprotein uptake occurs predominantly via scavenger receptors and is independent of cellular cholesterol homeostasis.[47] The progressive accumulation of FC by lesional macrophages may be explained by failure of one or more of the protective mechanisms as the atherosclerotic lesion progresses. It is well known that the ER is the site of ACAT-1–mediated esterification of FC and that lesion-resident macrophage foam cells accumulate large amounts of cholesterol esters. Thus, ER stress could potentially promote FC accumulation in lesion-resident macrophage foam cells by adversely affecting ACAT-1 activity and/or altering intracellular cholesterol trafficking. Because activation of SREBPs, ER-resident transcription factors responsible for the induction of cholesterol and triglyceride biosynthesis genes, is induced by ER stress,[27,48] pathophysiological conditions known to elicit ER stress could potentially mediate FC levels in lesion-resident macrophage foam cells.

Under normal cellular conditions, the UPR coordinately enhances cell survival by ensuring that the adverse effects of ER stress are dealt with in a timely and efficient manner. It is likely, therefore, that activation of the UPR in early-lesion–resident macrophages would initially provide a cytoprotective advantage; however, prolonged or severe ER stress can result in apoptotic cell death through the activation of multiple ER-specific proapoptotic factors, including CHOP, caspase-12, and TDAG51.[23,29,49,50] In support of this concept, prolonged ER stress in hypertrophic and failing hearts induces cardiac myocyte apoptosis.[51] Excess accumulation of FC is thought to be an important factor mediating macrophage foam cell death,[22] and recent studies have demonstrated that FC loading in cultured macrophages results in ER stress-induced apoptotic cell death.[23] FC-induced apoptotic cell death was attenuated in CHOP-deficient macrophages, and CHOP was markedly elevated in advanced atherosclerotic lesions from apoE$^{-/-}$ mice, which suggests that activation of the CHOP arm of the UPR is the key signaling step in cholesterol-induced apoptosis in macrophages.[23] In fatty streaks, we observed a significant accumulation of FC and lipid droplets, as well as immunostaining for the proapoptotic factors CHOP and TDAG51, in macrophage foam cells. Surprisingly, there was no evidence of apoptotic cell death despite the expression of CHOP and TDAG51. Apoptosis was observed only in advanced atherosclerotic lesions, which

suggests that the activation of additional cellular mediators, including Bax, p53, and Fas ligand,[14–17] and/or pathways contributes to macrophage apoptosis during atherosclerotic lesion development. Indeed, recent findings by I. Tabas, MD, PhD, and colleagues (written communication, March 2005) suggest that FC-induced macrophage apoptosis involves a 2-hit mechanism involving p38-induced UPR activation and type A scavenger receptor engagement. However, we were unable to determine whether the accumulation of intracellular FC in macrophages led to an increase in ER membrane FC, a prerequisite for apoptotic cell death.[23]

In summary, we have demonstrated that markers of ER stress and UPR activation are markedly increased in macrophages from both early and advanced atherosclerotic lesions. Although accumulation of FC and lipid was observed in the majority of early-lesion–resident macrophage foam cells, there was no evidence of apoptotic cell death at this stage. ER stress, FC accumulation, and apoptotic cell death were observed in macrophage foam cells from advanced atherosclerotic lesions, which suggests that other pathophysiological conditions in addition to FC or the activation of additional cellular pathways are required for the initiation of macrophage apoptosis. Given that prolonged or severe ER stress contributes to the pathogenesis of a number of human diseases, including diabetes, Alzheimer's disease, and Parkinson's disease,[52] our findings suggest that atherosclerotic lesion development likely is mediated in part by ER stress and activation of the UPR.

Acknowledgments

This work was supported in part by research grants to Dr Austin from the Heart and Stroke Foundation of Ontario (T-5385), the Canadian Institutes of Health Research (MOP-67116), and the Ontario Research and Development Challenge Fund. Dr Austin is a Career Investigator of the Heart and Stroke Foundation of Ontario (C/I-4763). We thank Drs Ira Tabas and Tracie De Vries-Seimon, Columbia University, New York, NY, for helpful discussions.

References

1. Stary HC, Chandler AB, Glagov S, Guyton JR, Insull W Jr, Rosenfeld ME, Schaffer SA, Schwartz CJ, Wagner WD, Wissler RW. A definition of initial, fatty streak, and intermediate lesions of atherosclerosis: a report from the Committee on Vascular Lesions of the Council on Arteriosclerosis, American Heart Association. *Circulation*. 1994;89:2462–2478.
2. Virmani R, Kolodgie FD, Burke AP, Farb A, Schwartz SM. Lessons from sudden coronary death: a comprehensive morphological classification scheme for atherosclerotic lesions. *Arterioscler Thromb Vasc Biol*. 2000; 20:1262–1275.
3. Stary HC, Chandler AB, Dinsmore RE, Fuster V, Glagov S, Insull W Jr, Rosenfeld ME, Schwartz CJ, Wagner WD, Wissler RW. A definition of advanced types of atherosclerotic lesions and a histological classification of atherosclerosis; a report from the Committee on Vascular Lesions of the Council on Arteriosclerosis, American Heart Association. *Circulation*. 1995;92:1355–1374.
4. Fuster V. Lewis A. Conner Memorial Lecture: mechanisms leading to myocardial infarction: insights from studies of vascular biology. *Circulation*. 1994;90:2126–2146.
5. Lee RT, Libby P. The unstable atheroma. *Arterioscler Thromb Vasc Biol*. 1997;17:1859–1867.
6. Falk E, Shah PK, Fuster V. Coronary plaque disruption. *Circulation*. 1995;92:657–671.
7. Kockx MM, De Meyer GR, Muhring J, Bult H, Bultinck J, Herman AG. Distribution of cell replication and apoptosis in atherosclerotic plaques of cholesterol-fed rabbits. *Atherosclerosis*. 1996;120:115–124.
8. Isner JM, Kearney M, Bortman S, Passeri J. Apoptosis in human atherosclerosis and restenosis. *Circulation*. 1995;91:2703–2711.
9. Hegyi L, Skepper JN, Cary NR, Mitchinson MJ. Foam cell apoptosis and the development of the lipid core of human atherosclerosis. *J Pathol*. 1996;180:423–429.
10. Kockx MM, Herman AG. Apoptosis in atherosclerosis: beneficial or detrimental? *Cardiovasc Res*. 2000;45:736–746.
11. Tedgui A, Mallat Z. Apoptosis as a determinant of atherothrombosis. *Thromb Haemost*. 2001;86:420–426.
12. Salvayre R, Auge N, Benoist H, Negre-Salvayre A. Oxidized low-density lipoprotein-induced apoptosis. *Biochim Biophys Acta*. 2002;1585: 213–221.
13. Hegyi L, Hardwick SJ, Siow RC, Skepper JN. Macrophage death and the role of apoptosis in human atherosclerosis. *J Hematother Stem Cell Res*. 2001;10:27–42.
14. van Vlijmen BJ, Gerritsen G, Franken AL, Boesten LS, Kockx MM, Gijbels MJ, Vierboom MP, van Eck M, van De Water B, van Berkel TJ, Havekes LM. Macrophage p53 deficiency leads to enhanced atherosclerosis in APOE*3-Leiden transgenic mice. *Circ Res*. 2001;88:780–786.
15. Branen L, Hovgaard L, Nitulescu M, Bengtsson E, Nilsson J, Jovinge S. Inhibition of tumor necrosis factor-α reduces atherosclerosis in apolipoprotein E knockout mice. *Arterioscler Thromb Vasc Biol*. 2004;24: 2137–2142.
16. Liu J, Thewke DP, Su YR, Linton MF, Fazio S, Sinensky MS. Reduced macrophage apoptosis is associated with accelerated atherosclerosis in low-density lipoprotein receptor-null mice. *Arterioscler Thromb Vasc Biol*. 2005;25:174–179.
17. Yang J, Sato K, Aprahamian T, Brown NJ, Hutcheson J, Bialik A, Perlman H, Walsh K. Endothelial overexpression of Fas ligand decreases atherosclerosis in apolipoprotein E–deficient mice. *Arterioscler Thromb Vasc Biol*. 2004;24:1466–1473.
18. Lundberg B. Chemical composition and physical state of lipid deposits in atherosclerosis. *Atherosclerosis*. 1985;56:93–110.
19. Small DM. George Lyman Duff memorial lecture: progression and regression of atherosclerotic lesions: insights from lipid physical biochemistry. *Arteriosclerosis*. 1988;8:103–129.
20. Kruth HS, Fry DL. Histochemical detection and differentiation of free and esterified cholesterol in swine atherosclerosis using filipin. *Exp Mol Pathol*. 1984;40:288–294.
21. Ball RY, Stowers EC, Burton JH, Cary NR, Skepper JN, Mitchinson MJ. Evidence that the death of macrophage foam cells contributes to the lipid core of atheroma. *Atherosclerosis*. 1995;114:45–54.
22. Tabas I. Consequences of cellular cholesterol accumulation: basic concepts and physiological implications. *J Clin Invest*. 2002;110: 905–911.
23. Feng B, Yao PM, Li Y, Devlin CM, Zhang D, Harding HP, Sweeney M, Rong JX, Kuriakose G, Fisher EA, Marks AR, Ron D, Tabas I. The endoplasmic reticulum is the site of cholesterol-induced cytotoxicity in macrophages. *Nat Cell Biol*. 2003;5:781–792.
24. Zinszner H, Kuroda M, Wang X, Batchvarova N, Lightfoot RT, Remotti H, Stevens JL, Ron D. CHOP is implicated in programmed cell death in response to impaired function of the endoplasmic reticulum. *Genes Dev*. 1998;12:982–995.
25. Paigen B, Morrow A, Holmes PA, Mitchell D, Williams RA. Quantitative assessment of atherosclerotic lesions in mice. *Atherosclerosis*. 1987;68: 231–240.
26. Kockx MM, Muhring J, Bortier H, De Meyer GR, Jacob W. Biotin- or digoxigenin-conjugated nucleotides bind to matrix vesicles in atherosclerotic plaques. *Am J Pathol*. 1996;148:1771–1777.
27. Werstuck GH, Lentz SR, Dayal S, Hossain GS, Sood SK, Shi YY, Zhou J, Maeda N, Krisans SK, Malinow MR, Austin RC. Homocysteine-induced endoplasmic reticulum stress causes dysregulation of the cholesterol and triglyceride biosynthetic pathways. *J Clin Invest*. 2001;107: 1263–1273.
28. Zhou J, Werstuck GH, Lhotak S, de Koning AB, Sood SK, Hossain GS, Moller J, Ritskes-Hoitinga M, Falk E, Dayal S, Lentz SR, Austin RC. Association of multiple cellular stress pathways with accelerated atherosclerosis in hyperhomocysteinemic apolipoprotein E–deficient mice. *Circulation*. 2004;110:207–213.
29. Hossain GS, van Thienen JV, Werstuck GH, Zhou J, Sood SK, Dickhout JG, de Koning AB, Tang D, Wu D, Falk E, Poddar R, Jacobsen DW, Zhang K, Kaufman RJ, Austin RC. TDAG51 is induced by homocysteine, promotes detachment-mediated programmed cell death, and contributes to the development of atherosclerosis in hyperhomocysteinemia. *J Biol Chem*. 2003;278:30317–30327.

30. Yoshida H, Matsui T, Yamamoto A, Okada T, Mori K. XBP1 mRNA is induced by ATF6 and spliced by IRE1 in response to ER stress to produce a highly active transcription factor. *Cell*. 2001;107:881–891.
31. Lee AH, Iwakoshi NN, Glimcher LH. XBP-1 regulates a subset of endoplasmic reticulum resident chaperone genes in the unfolded protein response. *Mol Cell Biol*. 2003;23:7448–7459.
32. Zhou J, Moller J, Danielsen CC, Bentzon J, Ravn HB, Austin RC, Falk E. Dietary supplementation with methionine and homocysteine promotes early atherosclerosis but not plaque rupture in ApoE-deficient mice. *Arterioscler Thromb Vasc Biol*. 2001;21:1470–1476.
33. Zhou J, Moller J, Ritskes-Hoitinga M, Larsen ML, Austin RC, Falk E. Effects of vitamin supplementation and hyperhomocysteinemia on atherosclerosis in apoE-deficient mice. *Atherosclerosis*. 2003;168:255–262.
34. Hofmann MA, Lalla E, Lu Y, Gleason MR, Wolf BM, Tanji N, Ferran LJ Jr, Kohl B, Rao V, Kisiel W, Stern DM, Schmidt AM. Hyperhomocysteinemia enhances vascular inflammation and accelerates atherosclerosis in a murine model. *J Clin Invest*. 2001;107:675–683.
35. Wang H, Jiang X, Yang F, Gaubatz JW, Ma L, Magera MJ, Yang X, Berger PB, Durante W, Pownall HJ, Schafer AI. Hyperhomocysteinemia accelerates atherosclerosis in cystathionine beta-synthase and apolipoprotein E double knock-out mice with and without dietary perturbation. *Blood*. 2003;101:3901–3907.
36. Boushey CJ, Beresford SA, Omenn GS, Motulsky AG. A quantitative assessment of plasma homocysteine as a risk factor for vascular disease: probable benefits of increasing folic acid intakes. *JAMA*. 1995;274:1049–1057.
37. Eikelboom JW, Lonn E, Genest J Jr, Hankey G, Yusuf S. Homocyst(e)ine and cardiovascular disease: a critical review of the epidemiologic evidence. *Ann Intern Med*. 1999;131:363–375.
38. Outinen PA, Sood SK, Liaw PCY, Sarge KD, Maeda N, Hirsh J, Ribau J, Podor TJ, Weitz JI, Austin RC. Characterization of the stress-inducing effects of homocysteine. *Biochem J*. 1998;332:213–221.
39. Reddy RK, Mao C, Baumeister P, Austin RC, Kaufman RJ, Lee AS. Endoplasmic reticulum chaperone protein GRP78 protects cells from apoptosis induced by topoisomerase inhibitors: role of ATP binding site in suppression of caspase-7 activation. *J Biol Chem*. 2003;278:20915–20924.
40. Watson LM, Chan AK, Berry LR, Li J, Sood SK, Dickhout JG, Xu L, Werstuck GH, Bajzar L, Klamut HJ, Austin RC. Overexpression of the 78-kDa glucose-regulated protein/immunoglobulin-binding protein (GRP78/BiP) inhibits tissue factor procoagulant activity. *J Biol Chem*. 2003;278:17438–17447.
41. Iwakoshi NN, Lee AH, Vallabhajosyula P, Otipoby KL, Rajewsky K, Glimcher LH. Plasma cell differentiation and the unfolded protein response intersect at the transcription factor XBP-1. *Nat Immunol*. 2003;4:321–329.
42. Lusis AJ. Atherosclerosis. *Nature*. 2000;407:233–241.
43. Kawahara K, Oyadomari S, Gotoh T, Kohsaka S, Nakayama H, Mori M. Induction of CHOP and apoptosis by nitric oxide in p53-deficient microglial cells. *FEBS Lett*. 2001;506:135–139.
44. Oyadomari S, Takeda K, Takiguchi M, Gotoh T, Matsumoto M, Wada I, Akira S, Araki E, Mori M. Nitric oxide–induced apoptosis in pancreatic beta cells is mediated by the endoplasmic reticulum stress pathway. *Proc Natl Acad Sci U S A*. 2001;98:10845–10850.
45. Chen J, Kuhlencordt P, Urano F, Ichinose H, Astern J, Huang PL. Effects of chronic treatment with L-arginine on atherosclerosis in apoE knockout and apoE/inducible NO synthase double-knockout mice. *Arterioscler Thromb Vasc Biol*. 2003;23:97–103.
46. Reddy RK, Dubeau L, Kleiner H, Parr T, Nichols P, Ko B, Dong D, Ko H, Mao C, DiGiovanni J, Lee AS. Cancer-inducible transgene expression by the Grp94 promoter: spontaneous activation in tumors of various origins and cancer-associated macrophages. *Cancer Res*. 2002;62:7207–7212.
47. Vainio S, Ikonen E. Macrophage cholesterol transport: a critical player in foam cell formation. *Ann Med*. 2003;35:146–155.
48. Ji C, Kaplowitz N. Betaine decreases hyperhomocysteinemia, endoplasmic reticulum stress, and liver injury in alcohol-fed mice. *Gastroenterology*. 2003;124:1488–1499.
49. Nakagawa T, Zhu H, Morishima N, Li E, Xu J, Yankner BA, Yuan J. Caspase-12 mediates endoplasmic-reticulum-specific apoptosis and cytotoxicity by amyloid-β. *Nature*. 2000;403:98–103.
50. Oyadomari S, Araki E, Mori M. Endoplasmic reticulum stress-mediated apoptosis in pancreatic beta-cells. *Apoptosis*. 2002;7:335–345.
51. Okada K, Minamino T, Tsukamoto Y, Liao Y, Tsukamoto O, Takashima S, Hirata A, Fujita M, Nagamachi Y, Nakatani T, Yutani C, Ozawa K, Ogawa S, Tomoike H, Hori M, Kitakaze M. Prolonged endoplasmic reticulum stress in hypertrophic and failing heart after aortic constriction: possible contribution of endoplasmic reticulum stress to cardiac myocyte apoptosis. *Circulation*. 2004;110:705–712.
52. Kaufman RJ. Orchestrating the unfolded protein response in health and disease. *J Clin Invest*. 2002;110:1389–1398.

Activation of the Unfolded Protein Response Occurs at All Stages of Atherosclerotic Lesion Development in Apolipoprotein E–Deficient Mice

Ji Zhou, Sárka Lhoták, Brooke A. Hilditch and Richard C. Austin

Circulation. 2005;111:1814-1821; originally published online April 4, 2005;
doi: 10.1161/01.CIR.0000160864.31351.C1
Circulation is published by the American Heart Association, 7272 Greenville Avenue, Dallas, TX 75231

Print ISSN: 0009-7322. Online ISSN: 1524-4539